

*Swift* J2058.4+0516: DISCOVERY OF A POSSIBLE SECOND RELATIVISTIC TIDAL DISRUPTION FLARE?

S. BRADLEY CENKO<sup>1</sup>, HANS A. KRIMM<sup>2,3</sup>, ASSAF HOESH<sup>4</sup>, ARNE RAU<sup>5</sup>, DALE A. FRAIL<sup>6</sup>, JAMIE A. KENNEA<sup>7</sup>, ANDREW J. LEVAN<sup>8</sup>, STEPHEN T. HOLLAND<sup>9</sup>, NATHANIEL R. BUTLER<sup>1,10</sup>, ROBERT M. QUIMBY<sup>4</sup>, JOSHUA S. BLOOM<sup>1</sup>, ALEXEI V. FILIPPENKO<sup>1</sup>, AVISHAY GAL-YAM<sup>11</sup>, JOCHEN GREINER<sup>5</sup>, S. R. KULKARNI<sup>4</sup>, ERAN O. OFEK<sup>4</sup>, FELIPE OLIVARES E.<sup>5</sup>, PATRICIA SCHADY<sup>5</sup>, JEFFREY M. SILVERMAN<sup>1</sup>, NIAL R. TANVIR<sup>12</sup>, AND DONG XU<sup>11</sup>

Draft version August 29, 2018

ABSTRACT

We report the discovery by the *Swift* hard X-ray monitor of the transient source *Swift* J2058.4+0516 (*Sw* J2058+05). Our multi-wavelength follow-up campaign uncovered a long-lived (duration  $\gtrsim$  months), luminous X-ray ( $L_{X,\text{iso}} \approx 3 \times 10^{47}$  erg s<sup>-1</sup>) and radio ( $\nu L_{\nu,\text{iso}} \approx 10^{42}$  erg s<sup>-1</sup>) counterpart. The associated optical emission, however, from which we measure a redshift of 1.1853, is relatively faint, and this is not due to a large amount of dust extinction in the host galaxy. Based on numerous similarities with the recently discovered GRB 110328A / *Swift* J164449.3+573451 (*Sw* J1644+57), we suggest that *Sw* J2058+05 may be the second member of a new class of relativistic outbursts resulting from the tidal disruption of a star by a supermassive black hole. If so, the relative rarity of these sources (compared with the expected rate of tidal disruptions) implies that either these outflows are extremely narrowly collimated ( $\theta < 1^\circ$ ), or only a small fraction of tidal disruptions generate relativistic ejecta. Analogous to the case of long-duration gamma-ray bursts and core-collapse supernovae, we speculate that rapid spin of the black hole may be a necessary condition to generate the relativistic component. Alternatively, if powered by gas accretion (i.e., an active galactic nucleus [AGN]), *Sw* J2058+05 would seem to represent a new mode of variability in these sources, as the observed properties appear largely inconsistent with known classes of AGNs capable of generating relativistic jets (blazars, narrow-line Seyfert 1 galaxies).

*Subject headings:* X-rays: bursts — accretion — galaxies: nuclei — black hole physics — X-rays: individual (*Sw* J1644+57)

1. INTRODUCTION

The recent discovery of the transient source GRB 110328A / *Swift* J164449.3+573451 (*Sw* J1644+57) has unveiled an entirely new class of high-energy outbursts (Levan et al. 2011; Burrows et al. 2011; Zauderer et al. 2011). Like long-duration gamma-ray bursts (GRBs), the outburst was believed to mark the birth of a relativistic jet, generating luminous X-ray and radio emission. However, the central engine powering *Sw* J1644+57 was the super-massive ( $M_{\text{BH}} \lesssim 10^7 M_\odot$ ) black hole in the nucleus of an otherwise normal (i.e., nonactive) galaxy (Bloom et al. 2011). While not conclusive, the observed emission may result from the tidal disruption (Rees 1988) of a star (or white dwarf; Krolik & Piran 2011) pass-

ing too close to the central black hole (Bloom et al. 2011; Burrows et al. 2011; Zauderer et al. 2011; Cannizzo et al. 2011). A number of tidal disruption flare (TDF) candidates have been previously identified at longer wavelengths (e.g., Renzini et al. 1995; Bade et al. 1996; Komossa & Greiner 1999; Greiner et al. 2000; Donley et al. 2002; Gezari et al. 2006, 2008, 2009; Esquej et al. 2007, 2008; Maksym et al. 2010; van Velzen et al. 2011; Cenko et al. 2012). But the robust inference of a newly born relativistic jet, and the insights into the accretion and jet-formation processes provided therein, clearly distinguish *Sw* J1644+57 from previous TDF candidates.

In this work, we report on a recently discovered high-energy transient, *Swift* J2058.4+0516 (*Sw* J2058+05). Remarkably, *Sw* J2058+05 shares many of the properties that made *Sw* J1644+57 such an exceptional event, in particular (1) a long-lived (duration  $\gtrsim$  months), super-Eddington ( $L_{X,\text{iso}} \approx 3 \times 10^{47}$  erg s<sup>-1</sup>) X-ray outburst; (2) a luminous radio counterpart, indicating the presence of relativistic ( $\Gamma \gtrsim 2$ ) ejecta; and (3) relatively faint ( $M_U \approx -22.7$  mag) optical emission. If future observations are able to establish an astrometric association with the nucleus of the redshift  $z = 1.1853$  host galaxy, and also continue to suggest that this galaxy does not harbor an active galactic nucleus (AGN), we may have identified a second member of this new class of relativistic TDFs. Alternatively, several classes of AGNs are known to generate relativistic jets (blazars, narrow-line Seyfert 1 [NLS1] galaxies). If *Sw* J2058+05 is shown to result from an AGN (e.g., via repeated outbursts over the coming years), we would have uncovered yet another unique example of the already diverse phenomenology of variability from active galaxies.

Throughout this work, we adopt a standard  $\Lambda$ CDM cosmology with  $H_0 = 71$  km s<sup>-1</sup> Mpc<sup>-1</sup>,  $\Omega_m = 0.27$ , and  $\Omega_\Lambda = 1 - \Omega_m =$

<sup>1</sup> Department of Astronomy, University of California, Berkeley, CA 94720-3411, USA

<sup>2</sup> CRESST and NASA Goddard Space Flight Center, Greenbelt, MD 20771, USA

<sup>3</sup> Universities Space Research Association, 10211 Wincopin Circle, Suite 500, Columbia, MD 21044, USA

<sup>4</sup> Division of Physics, Mathematics, and Astronomy, California Institute of Technology, Pasadena, CA 91125, USA

<sup>5</sup> Max-Planck Institute for Extraterrestrial Physics, Giessenbachstrasse 1, Garching 85748, Germany

<sup>6</sup> National Radio Astronomy Observatory, P.O. Box 0, Socorro, NM 87801, USA

<sup>7</sup> Department of Astronomy & Astrophysics, The Pennsylvania State University, 525 Davey Laboratory, University Park, PA 16802, USA

<sup>8</sup> Department of Physics, University of Warwick, Coventry, CV4 7AL, UK

<sup>9</sup> Space Telescope Science Institute, 3700 San Martin Drive, Baltimore, MD 21218, USA

<sup>10</sup> Einstein Fellow

<sup>11</sup> Department of Particle Physics and Astrophysics, Faculty of Physics, The Weizmann Institute of Science, Rehovot 76100, Israel

<sup>12</sup> Department of Physics and Astronomy, University of Leicester, University Road, Leicester LE1 7RH, UK

Electronic address: cenko@astro.berkeley.edu

0.73 (Spergel *et al.* 2007). All quoted uncertainties are  $1\sigma$  (68%) confidence intervals unless otherwise noted, and UT times are used throughout. Reported magnitudes are in the AB system (Oke & Gunn 1983).

## 2. DISCOVERY AND OBSERVATIONS

### 2.1. *Swift*-BAT Hard X-ray Monitor Discovery

*Sw* J2058+05 was discovered by the Burst Alert Telescope (BAT; Barthelmy *et al.* 2005) on the *Swift* satellite (Gehrels *et al.* 2004) as part of the hard X-ray monitor's automated transient search. It first reached the  $6\sigma$  discovery threshold in a 4 d integration covering the time period 2011 May 17–20, with a 15–50 keV count rate of  $0.0044 \pm 0.0006 \text{ counts s}^{-1} \text{ cm}^{-2}$  (Krimm *et al.* 2011)<sup>13</sup>. No significant emission was detected from this location after 2011 June 2. The resulting BAT (15–50 keV) light curve is plotted in the top panel of Figure 1.

The observed BAT count rate is too low to measure statistically significant variations on time scales shorter than 4 d, or to constrain the hard X-ray spectrum. A search of transient monitor data on the same 4 d time scale back to 2005 February shows no previous activity from the source with a  $3\sigma$  count rate limit of  $< 0.003 \text{ count s}^{-1} \text{ cm}^{-2}$ .

### 2.2. X-rays

To confirm this discovery, we requested a *Swift* target-of-opportunity (ToO) observation, which began at 21:56 on 2011 May 28. Data obtained by the X-ray Telescope (XRT; Burrows *et al.* 2005) were reduced using the online analysis tools of Evans *et al.* (2009), and XRT spectra were fitted using `xspec12.6`<sup>14</sup>. After correcting the XRT astrometry following Goad *et al.* (2008), we identified a bright point source at (J2000.0) coordinates  $\alpha = 20^{\text{h}}58^{\text{m}}19.85^{\text{s}}$ ,  $\delta = +05^{\circ}13'33''.0$ , with a 90% localization radius of  $1''.7$ . The XRT continued to monitor *Sw* J2058+05; the resulting 0.3–10 keV light curve is plotted in the middle panel of Figure 1.

Superimposed on the secular decline (reasonably well described by a power law:  $L_X \propto t^{-2.2}$ ), the X-ray light curve shows some degree of variability on relatively short time scales (compared to the time since discovery). The most significant flaring is detected on 2011 June 2, with a change in flux of a factor of 1.5 occurring on a time scale of  $\delta t \approx 10^4 \text{ s}$ . No significant variability is detected on shorter time scales; however, given the signal-to-noise ratio (SNR), we are not sensitive to similar variations (i.e., factor of 2) on time scales shorter than  $\sim 10^3 \text{ s}$ .

The average photon-counting mode spectrum is reasonably well described by an absorbed power law with photon index  $\Gamma = 1.61 \pm 0.12$  and  $N_{\text{H,host}} = (2.6 \pm 1.6) \times 10^{21} \text{ cm}^{-2}$  ( $\chi^2 = 65.95$  for 54 degrees of freedom, d.o.f.; see Butler & Kocevski 2007 for details of the spectral analysis). Using this time-averaged spectrum, we find that the peak (unabsorbed) 0.3–10 keV flux is  $f_X \approx 7.9 \times 10^{-11} \text{ erg cm}^{-2} \text{ s}^{-1}$ . The requirement for absorption in excess of the Galactic value ( $N_{\text{H,Gal}} = 6.5 \times 10^{20}$ ; Kalberla *et al.* 2005) is only significant at the  $3.2\sigma$  level. Interestingly, the time-resolved hardness ratio is inversely correlated with the source flux (Figure 1), a behavior commonly seen in Galactic black hole binaries (e.g., Remillard & McClintock 2006).

<sup>13</sup> Though not precisely constrained, we hereafter refer to the discovery time ( $t_0$ ) as 00:00 on 2011 May 17 (MJD = 55698).

<sup>14</sup> See <http://heasarc.gsfc.nasa.gov/docs/xanadu/xspec/>.

To improve the astrometric precision of the X-ray localization, we obtained ToO observations of *Sw* J2058+05 with the High Resolution Camera (HRC; Murray *et al.* 1997) on the *Chandra* X-ray Observatory. Observations began at 14:51 on 2011 June 22, for a total live exposure of 5.2 ks. *Sw* J2058+05 is well detected with (J2000.0) coordinates  $\alpha = 20^{\text{h}}58^{\text{m}}19.90^{\text{s}}$ ,  $\delta = +05^{\circ}13'32''.0$ , and an astrometric uncertainty of  $0''.4$  (Figure 2; the lack of additional point sources in the HRC image precludes us from improving the native *Chandra* astrometric precision). The X-ray flux shows weak evidence ( $1.5\sigma$ ) for a decline over the course of the entire observation, but no statistically significant variability on shorter time scales.

Finally, we note that the location of *Sw* J2058+05 was observed on 2000 March 16 by the Position Sensitive Proportional Counters (PSPC) onboard *ROSAT* as part of the All-Sky Survey (Voges *et al.* 1999). No sources are detected in the field to a limit of  $f_X(0.1\text{--}2.4 \text{ keV}) < 10^{-13} \text{ erg cm}^{-2} \text{ s}^{-1}$ , several orders of magnitude fainter than the observed outburst.

### 2.3. UV/Optical/NIR Photometry

Following the discovery of the X-ray counterpart, we initiated a campaign to observe *Sw* J2058+05 in the ultraviolet (UV), optical, and near-infrared (NIR), with the *Swift* Ultraviolet-Optical Telescope (UVOT; Roming *et al.* 2005), the 7-channel imager GROND (Greiner *et al.* 2008) mounted on the 2.2 m telescope at La Silla Observatory, the Low Resolution Imaging Spectrometer (LRIS; Oke *et al.* 1995) mounted on the 10 m Keck I telescope, the Wide-Field Camera (WFCAM) on the United Kingdom Infrared Telescope (UKIRT), and the Auxiliary-port Camera (ACAM) on the 4.2 m William Herschel Telescope. All observations were reduced following standard procedures and photometrically calibrated with respect to the 2 Micron All Sky Survey (2MASS; Skrutskie *et al.* 2006) in the NIR, Sloan Digital Sky Survey (SDSS; Abazajian *et al.* 2009) in the optical, and following Poole *et al.* (2008) for the UVOT.

The optical counterpart of *Sw* J2058+05 was first identified in our GROND imaging obtained on 2011 May 29 at (J2000.0) coordinates  $\alpha = 20^{\text{h}}58^{\text{m}}19.90^{\text{s}}$ ,  $\delta = +05^{\circ}13'32''.2$ , with an astrometric uncertainty of  $0''.2$  (radius; Rau *et al.* 2011a,b). The counterpart appears point-like in all our images, with the tightest constraints provided by our Keck/LRIS images on 2011 Jun 29 ( $0''.7$  seeing; Figure 2). Since discovery, we detect statistically significant fading in the bluer filters, but the degree of optical variability is much smaller than that observed in the X-rays. A full listing of our photometry is provided in Table 1, while the light curves are plotted in the bottom panel of Figure 1.

Pre-outburst imaging of the location of *Sw* J2058+05 was obtained on 2005 September 28 as part of SDSS. No source consistent with the location of *Sw* J2058+05 appears in the SDSS catalogs. Manually inspecting the images, we calculate  $3\sigma$  upper limits of  $u' > 21.9$ ,  $g' > 23.5$ ,  $r' > 23.5$ ,  $i' > 23.0$ , and  $z' > 21.7$  mag. The lack of a pre-existing counterpart in SDSS is indicative that the observed optical emission is dominated by transient light and not any underlying host galaxy.

### 2.4. Optical Spectroscopy

We obtained a series of optical spectra of *Sw* J2058+05 on 2011 June 1 with the Deep Imaging Multi-Object Spectrograph (DEIMOS; Faber *et al.* 2003) mounted on the 10 m Keck II telescope. The instrument was configured with the 600 lines  $\text{mm}^{-1}$  grating, providing spectral coverage over the region  $\lambda = 4500\text{--}9500 \text{ \AA}$  with a spectral resolution of 3.5 Å.

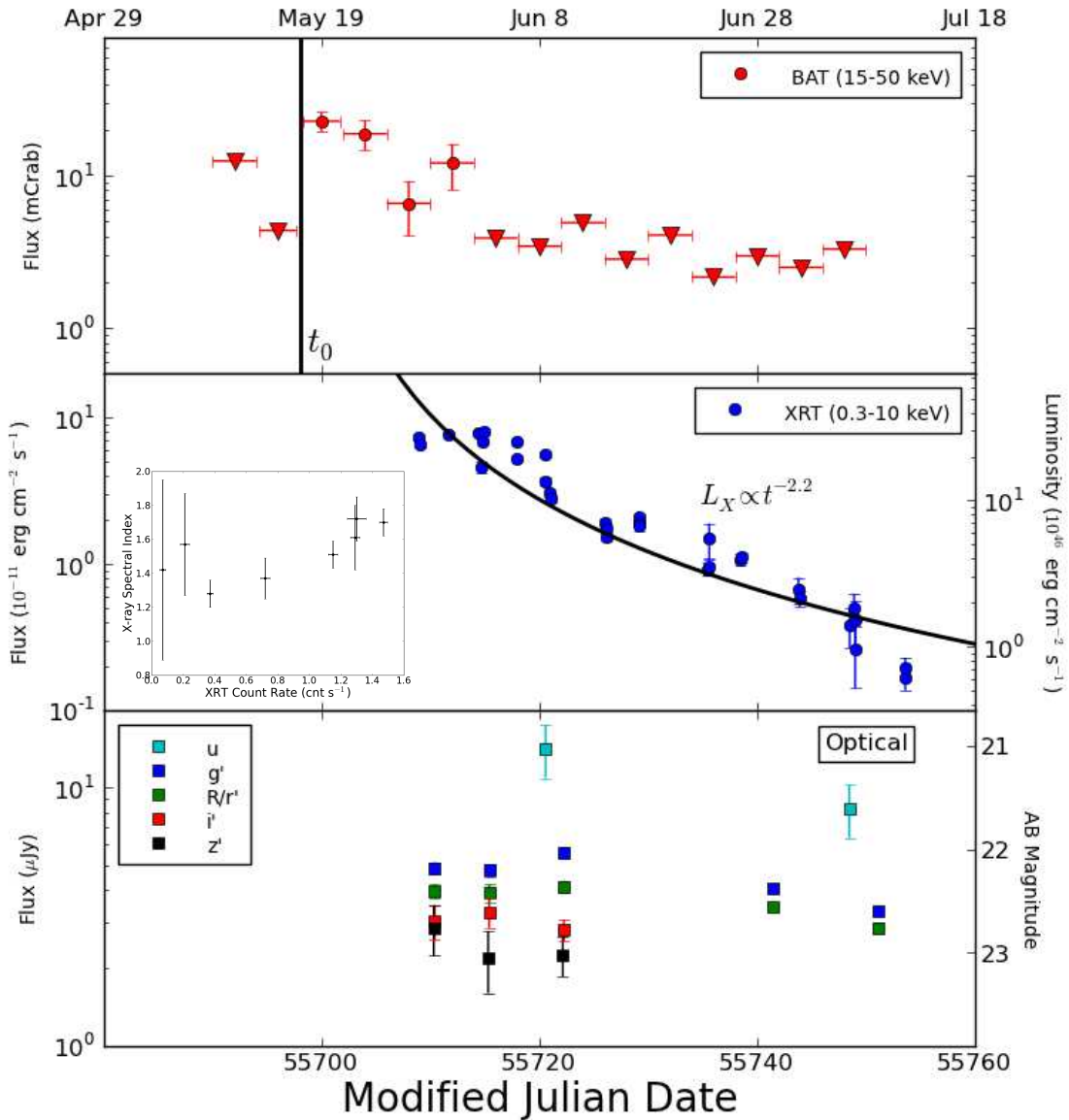


FIG. 1.— Hard X-ray (15–50 keV), X-ray (0.3–10 keV), and optical light curve of *Sw* J2058+05. The inset in the X-ray panels shows the derived power-law spectral index ( $\Gamma$ ) as a function of the X-ray count rate (i.e., flux). Inverted triangles represent  $3\sigma$  upper limits.

The spectra were optimally extracted (Horne 1986), and the rectification and sky subtraction were performed following the procedure described by Kelson (2003). The slit was oriented at the parallactic angle to minimize losses due to atmospheric dispersion (Filippenko 1982).

A portion of the resulting spectrum is plotted in Figure 3. Superimposed on a relatively blue continuum, we identify several strong (rest-frame equivalent width  $W_r \gtrsim 1 \text{ \AA}$ ) absorption features corresponding to Mg II  $\lambda\lambda 2796, 2803$ , Fe II  $\lambda 2600$ , Fe II  $\lambda 2587$ , Fe II  $\lambda 2383$ , and Fe II  $\lambda 2344$  at  $z = 1.1853 \pm 0.0004$ . Given the  $U$ -band detection ( $z \lesssim 2$  assuming  $\lambda_{Ly\alpha} \lesssim \lambda_U$ ), we assume this redshift corresponds to the host galaxy of *Sw* J2058+05. No other significant features are detected, either in emission or absorption, over the observed bandpass. Specifically, we limit the flux from [O II]  $\lambda 3727$  to be  $f < 3 \times 10^{-17} \text{ erg cm}^{-2} \text{ s}^{-1}$  ( $3\sigma$ ).

A second spectrum was obtained with Keck/LRIS on 2011 June 29, covering the wavelength range 3500–9500 Å. We find no significant evolution in either the shape of the continuum or the observed absorption features over this time period.

### 2.5. Radio

We observed the location of *Sw* J2058+05 with the NRAO Expanded Very Large Array (EVLA; Perley et al. 2011)<sup>15</sup> on 2011 June 29.36 and 2011 July 19.39. Observations were conducted in the C band (4–8 GHz) on June 29 and in the K (8–12 GHz) and X (18–26 GHz) bands on July 19. The array was in the A configuration for both epochs, and data were processed using standard routines in the AIPS environment.

<sup>15</sup> The National Radio Astronomy Observatory is a facility of the National Science Foundation operated under cooperative agreement by Associated Universities, Inc.

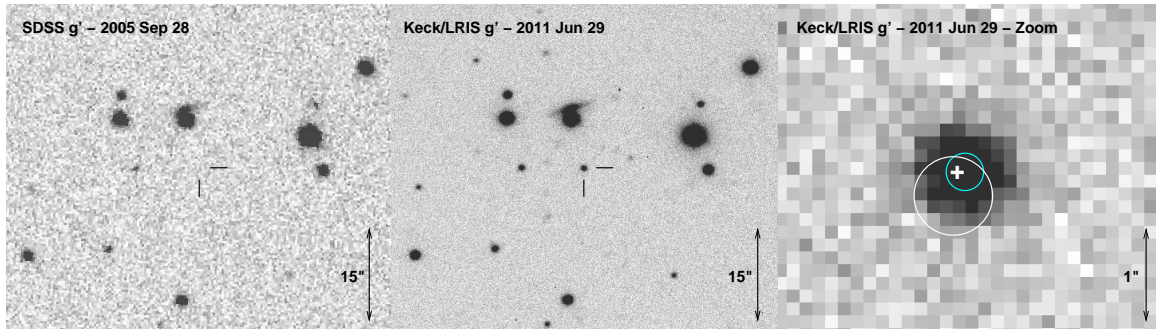


FIG. 2.— Optical finder chart for the field of *Sw* J2058+05. *Left*: Pre-outburst SDSS  $g'$  image. No emission is detected at the position of *Sw* J2058+05 (indicated with the black tick marks) to a limiting magnitude of  $g' > 23.5$  mag. *Middle*: Keck/LRIS  $g'$  image of the optical transient. The source appears point-like in this image ( $0''.7$  seeing). *Right*: Zoom-in of the Keck/LRIS image of the transient. The uncertainty in the astrometric tie for the optical frame (aligned with respect to 2MASS, which is reprojected onto the ICRS reference system) is indicated by the cyan circle ( $0''.2$  radius). The *Chandra*/HRC X-ray localization (based on the native *Chandra* astrometry, which is generated with respect to the ICRS) is plotted as the white circle ( $0''.4$  radius), while the EVLA radio position (50 mas uncertainty) is shown as the white cross. All three positions are entirely consistent. All images are oriented with north up and east to the left.

Within the EVLA field of view, we detect a single point source with (J2000.0) coordinates  $\alpha = 20^{\text{h}}58^{\text{m}}19.898^{\text{s}}$ ,  $\delta = +05^{\circ}13'32''.25$ , with an (absolute) astrometric uncertainty of 50 mas. We report the following flux densities: on June 29,  $f_{\nu}(\nu = 4.5 \text{ GHz}) = 0.88 \pm 0.05 \text{ mJy}$  and  $f_{\nu}(\nu = 7.9 \text{ GHz}) = 0.84 \pm 0.04 \text{ mJy}$ ; on July 19,  $f_{\nu}(\nu = 8.4 \text{ GHz}) = 1.34 \pm 0.04 \text{ mJy}$  and  $f_{\nu}(\nu = 22.5 \text{ GHz}) = 1.21 \pm 0.15 \text{ mJy}$ .

The EVLA localization is plotted as a cross in the right panel of Figure 2. Native EVLA astrometry is relative to the ICRS system, which we have also used for the optical (via the 2MASS point source catalog) and X-ray localizations (via the native *Chandra* pointing solution). All three positions are coincident, implying that the emission we are observing in different bandpasses all results from the same physical source.

This field had been observed previously by the VLA at 1.4 GHz, once on 1996 July 8 as part of the NRAO VLA Sky Survey (NVSS; Condon *et al.* 1998), and three times in 2009 (March 9, March 16, and May 9) as part of the Faint Images of the Radio Sky at Twenty-Centimeters (FIRST; Becker *et al.* 1995) survey. We inspected the images from these surveys and found no source at the position of *Sw* J2058+05, with  $3\sigma$  limits of  $f_{\nu} < 1.5 \text{ mJy}$  (NVSS) and  $0.38 \text{ mJy}$  (FIRST).

### 3. DISCUSSION

#### 3.1. Comparison to *Sw* J1644+57 and Known Classes of Active Galaxies

In Figure 4, we plot the X-ray and optical luminosity of *Sw* J2058+05 at an (observer-frame) time of  $\Delta t \approx 12 \text{ d}$  after discovery. For comparison, we also plot analogous measurements for a sample of long-duration GRB X-ray afterglows (at the same epoch post-burst), as well as nearby AGNs, more distant, luminous quasars from SDSS, and some of the most dramatically variable blazars *observed while in outburst*. With an isotropic X-ray luminosity  $L_{X,\text{iso}} \approx 3 \times 10^{47} \text{ erg s}^{-1}$ , *Sw* J2058+05 is much too luminous at this late time to result from a GRB. Yet with an absolute magnitude of  $M_U \approx -22.7$  mag, the observed optical emission is several orders of magnitude underluminous compared with the brightest X-ray quasars and blazars. Even compared with simultaneous X-ray and optical observations of the strongest high-energy flares from some of the best-known blazars (e.g., Markarian 501, Pian *et al.* 1998; 3C 279, Wehrle *et al.* 1998; Markarian 421, Fossati *et al.* 2008), the ratio of X-ray to optical luminosity appears to be quite unique. However, *Sw* J2058+05 occupies a nearly identical region of this phase space as *Sw* J1644+57.

This similarity is further reinforced when adding the ra-

dio observations to the broadband spectral energy distribution (SED). In Figure 5 we plot the SED of *Sw* J2058+05 at  $\Delta t \approx 43 \text{ d}$  after discovery, compared with analogous measurements for a sample of blazars, the most dramatically variable class of AGNs (and also known sources of relativistic jets; Urry & Padovani 1995; see §3.2). Blazars exhibit a well-defined luminosity “sequence” whereby the lower-frequency maximum of their double-peaked SED occurs at lower energies for more luminous sources (Fossati *et al.* 1998). While the radio and optical emission from *Sw* J2058+05 are comparable to those seen in low-luminosity blazars, the X-ray emission outshines even the brightest sources of this class. On the other hand, the SED of *Sw* J1644+57, at a time of  $\Delta t \approx 20 \text{ d}$ , provides a good match to the observed properties of *Sw* J2058+05 (particularly after correcting for the large but uncertain dust extinction from *Sw* J1644+57).

While the sequence plotted in Figure 5 may represent the ensemble properties of blazars as a class, individual sources may exhibit quite different behavior. During an outburst, blazar SEDs can undergo radical changes — for example, as a result of a rapid brightening in 1997, the low-energy (synchrotron) spectral peak in Markarian 501 shifted frequencies by approximately two orders of magnitude (Pian *et al.* 1998). We therefore also compare the observed SED of *Sw* J2058+05 with that of several high-energy outbursts from known blazars in Figure 6. Even when compared with these extreme cases, the ratio of the X-ray to optical flux observed in *Sw* J2058+05 stands out, being similar only to the broadband properties of *Sw* J1644+57.

The sole remaining defining characteristic of *Sw* J1644+57 is its association with the nucleus of a nonactive galaxy (Levan *et al.* 2011; Zauderer *et al.* 2011). At the current time, the observed optical emission from *Sw* J2058+05 appears to be dominated by the transient, and we have no constraints on the location of the host nucleus from pre-outburst observations. Future high-resolution observations, when the transient light has faded, should be able to constrain the transient-nucleus offset. That said, the detection of strong absorption features indicates that the line of sight penetrates a dense region of the host galaxy (as in the case of some GRBs).

Finally, we utilize the optical spectrum to search for evidence of past AGN activity. Like blazars, NLS1 galaxies are another subclass of AGNs that can sometimes power relativistic jets (e.g., Abdo *et al.* 2009b,a; Foschini *et al.* 2011; §3.2). Similarly, some NLS1 galaxies have been associated with luminous ( $L_X \approx 10^{44} \text{ erg s}^{-1}$ ) X-ray outbursts (e.g., Grupe *et al.*



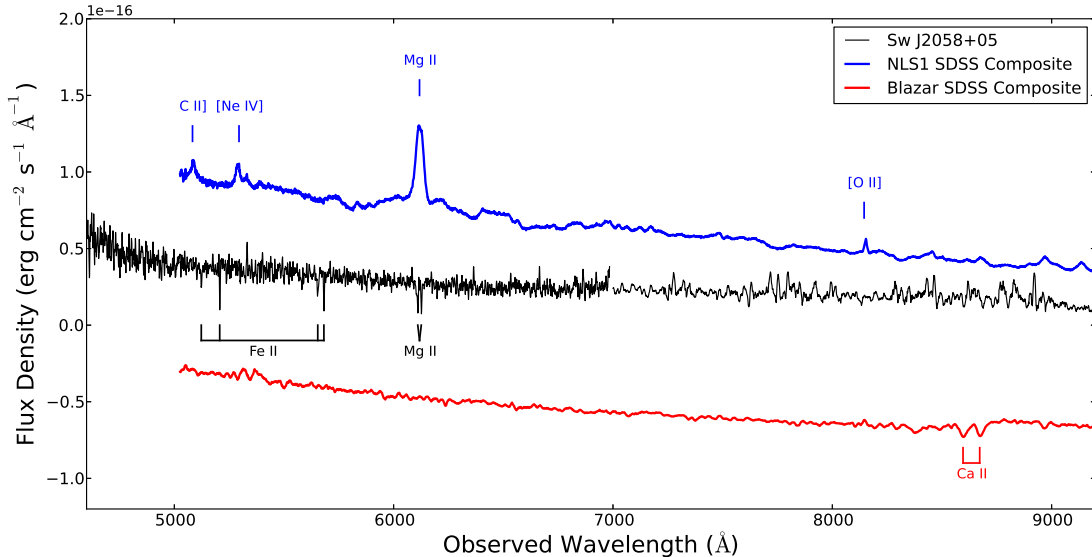


FIG. 3.— Keck/DEIMOS optical spectrum of *Sw* J2058+05 (black). The significant absorption features, corresponding to Mg II  $\lambda\lambda$ 2796, 2803, Fe II  $\lambda$ 2600, Fe II  $\lambda$ 2587, Fe II  $\lambda$ 2383, and Fe II  $\lambda$ 2344 at a common redshift of  $1.1853 \pm 0.0004$ , are marked. Also plotted is an average of the 478 known NLS1 galaxies (blue) and 68 blazars (red) at  $z > 0.5$  with spectra in SDSS. All but one of these NLS1 galaxies exhibit broad Mg II emission (as well as weaker C II), [Ne IV], and [O II]), which is entirely lacking from *Sw* J2058+05. While the blazars (by definition) lack strong emission features, most exhibit Ca II  $\lambda\lambda$ 3934, 3968 absorption, and none have Mg II detected in absorption. Note that the red-side spectrum of *Sw* J2058+05 (longward of  $\sim 7000$  Å) suffers from relatively poor night-sky subtraction, giving rise to apparent emission lines. Also, the weak emission features near 5300 Å in the blazar spectrum are likely to be noise.

1995; Brandt et al. 1995). In the case of *Sw* J1644+57, all of the detected emission lines were unresolved, and standard diagnostic diagrams revealed no evidence for ionization from a hidden (i.e., Compton thick) AGN (Levan et al. 2011; Zauderer et al. 2011). The larger redshift precludes such an analysis for *Sw* J2058+05, as the standard diagnostic lines do not fall in the optical bandpass.

However, we have compiled all of the available spectra from SDSS of known NLS1 galaxies (from the catalog of Véron-Cetty & Véron 2010) with  $z > 0.5$  (478 objects), and used these to create an NLS1 template. This composite spectrum is plotted alongside that of *Sw* J2058+05 in Figure 3. The template exhibits strong, broad emission from C II)  $\lambda$ 2324, [Ne IV]  $\lambda\lambda$ 2422, 2424, and in particular Mg II  $\lambda\lambda$ 2796, 2803. None of these emission lines are detected in our spectrum of *Sw* J2058+05. In fact, of the 478 known NLS1 galaxies in SDSS with  $z > 0.5$ , all but one have well-detected ( $> 3\sigma$ ) Mg II in emission. Unless exceedingly rare, the optical spectrum of *Sw* J2058+05 suggests that it is not an NLS1 galaxy.

We have furthermore performed a similar analysis with all known BL Lac sources from Véron-Cetty & Véron (2010) at  $z > 0.5$  in the SDSS archive (68 sources); the resulting median spectrum is shown in red in Figure 3. By definition, BL Lacs lack the bright emission features present in the spectra of NLS1 galaxies, and therefore they more closely resemble the observed spectrum of *Sw* J2058+05. However, BL Lac spectra do typically exhibit Ca II  $\lambda\lambda$ 3934, 3968 in absorption, which is lacking in *Sw* J2058+05, and not a single BL Lac in the SDSS database exhibits strong Mg II absorption. While we cannot entirely rule out a new mode of variability in a blazar, the unique SED and optical spectrum distinguish *Sw* J2058+05 from known members of this class as well.

### 3.2. Basic Physical Properties

We have shown in the previous section that *Sw* J2058+05 does not appear consistent with any known class of AGNs

(particularly blazars and NLS1). Based on the many similarities with *Sw* J1644+57, we can use the same arguments to derive the basic physical parameters for *Sw* J2058+05 (e.g., Bloom et al. 2011). From our NIR observations, we derive an upper limit on the host-galaxy absolute *V*-band magnitude of  $M_V \gtrsim -21$  mag (we have used an S0 galaxy template from Kinney et al. 1996 for the *K*-correction based on the lack of emission features in the optical spectrum). Applying the black hole mass vs. bulge luminosity (Magorrian et al. 1998) correlation from Lauer et al. (2007) and assuming a bulge-dominated system, we limit the mass of the putative central black hole to be  $M_{\text{BH}} \lesssim 2 \times 10^8 M_{\odot}$ .

Separately, the shortest observed X-ray variability time scale can be used to constrain the central black hole mass using causality arguments (e.g., Campana et al. 2011). For an observer-frame variability time scale of  $\delta t \lesssim 10^4$  s, we find  $M_{\text{BH}} \lesssim 5 \times 10^8 M_{\odot}$ . The most dramatic short time scale variability observed from *Sw* J1644+57 occurred at  $\Delta t \lesssim 10$  d (Bloom et al. 2011), before we commenced X-ray observations of *Sw* J2058+05. But even at late times, the X-ray light curve of *Sw* J2058+05 exhibits a degree of variability (changes of an order of magnitude on time scales of a few days) not seen in *Sw* J2058+05, suggesting an imperfect analogy between these two sources.

Finally, we can constrain the central mass using the black hole fundamental plane, a relationship between mass, X-ray luminosity, and radio luminosity (e.g., Gültekin et al. 2009). Application of this relation requires knowledge of the beaming fraction, for which we adopt a value of  $f_b \equiv (1 - \cos \theta) \approx 10^{-2}$  (see below). Following Miller & Gültekin (2011), we find  $M_{\text{BH}} \approx 5 \times 10^7 M_{\odot}$ ; however, we caution that the scatter in this relationship is even larger than that found in the black hole mass vs. bulge luminosity relation.

The derived black hole mass,  $M_{\text{BH}} \lesssim 10^8 M_{\odot}$ , is of vital importance for two main reasons. First, the tidal disruption of a solar-type star will only occur outside the event horizon for

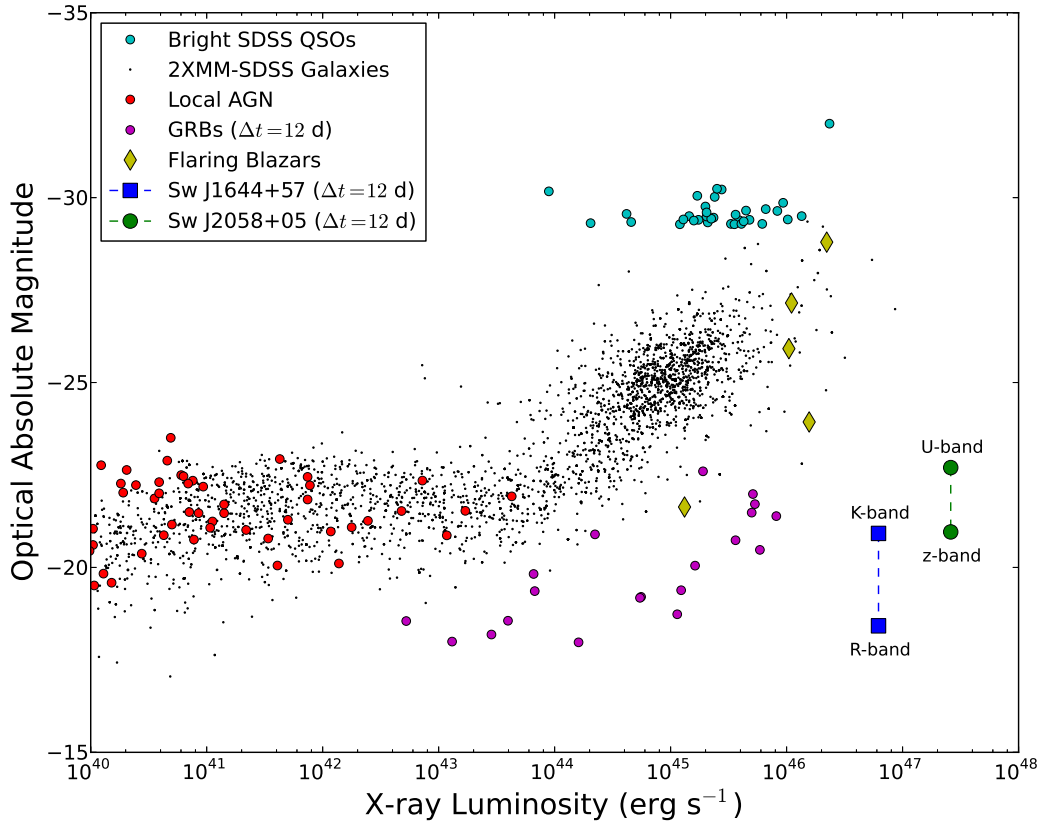


FIG. 4.— X-ray and optical luminosity of *Sw* J2058+05, compared with a sample of nearby active galaxies (red circles; Ho 2009), luminous quasars from SDSS (cyan circles), galaxies from SDSS with XMM counterparts (black dots; Pineau et al. 2011), long-duration GRB afterglows (extrapolated to a common epoch of  $\Delta t = 12$  d after the GRB trigger; Kann et al. 2010; Evans et al. 2009), and high-energy outbursts from known blazars (Markarian 501, Pian et al. 1998; PKS 2155-304, Foschini et al. 2007; PKS 0537-441, Pian et al. 2007; 3C 279, Wehrle et al. 1998; Markarian 421, Fossati et al. 2008). Compared with these sources (and at the same epoch post-discovery as the GRBs), both *Sw* J2058+05 and *Sw* J1644+57 exhibit extremely luminous X-ray emission, yet relatively faint optical emission. While for *Sw* J1644+57 this is to some extent due to dust extinction in the host galaxy (for which we have not corrected here), the blue UV/optical SED of *Sw* J2058+05 suggests at most a modest host-galaxy column density. We note that we have not K-corrected the absolute magnitudes reported here (aside from cosmological stretch) due to the relatively uncertain intrinsic SEDs. Adapted from Levan et al. (2011).

$M_{\text{BH}} \lesssim 2 \times 10^8 M_{\odot}$ . As such, if the origin of the accreting material is indeed the tidal disruption of a nondegenerate star (or more massive object), the mass of the central black hole in the host galaxy of *Sw* J2058+05 must be sufficiently small<sup>16</sup>. Future observations of the host, when the optical transient light has faded, should provide a significantly improved estimate of  $M_{\text{BH}}$ .

Second, for  $M_{\text{BH}} \lesssim 10^8 M_{\odot}$ , the observed X-ray emission exceeds the Eddington luminosity. In particular, the peak isotropic 0.3–10 keV X-ray luminosity of  $L_{\text{X,iso}} \approx 3 \times 10^{47} \text{ erg s}^{-1}$  exceeds the Eddington value by more than an order of magnitude. Given the long-lived nature of the central engine, this suggests the outflow is likely to be collimated with a beaming factor  $f_b \lesssim 10^{-1}$  (cf., Socrates 2011). An even larger degree of collimation is required to reconcile the observed rate of these outbursts with theoretical predictions for TDFs (§4).

More robust evidence for beaming is provided by the large radio luminosity. It is well known that the brightness tem-

perature of an incoherent radio source cannot exceed  $10^{11} \text{ K}$  for extended periods of time (Readhead 1994; Kulkarni et al. 1998). Utilizing this fact, we can derive a lower limit on the angular size of the radio-emitting region,  $\theta \gtrsim 14 \mu\text{as}$ . Assuming that the outflow commencement coincides with the hard X-ray discovery, this implies a mean expansion velocity of  $\beta \equiv v/c \geq 0.88$ , or a mildly relativistic expansion with  $\Gamma \geq 2.1$ . Furthermore, the radio emission will be collimated into a viewing angle  $\theta \lesssim 1/\Gamma$  due to relativistic beaming effects.

If we integrate over the X-ray light curve to date (2011 July 20), we find that *Sw* J2058+05 has emitted a total 0.3–10 keV fluence of  $S_{\text{X}} \approx 1.0 \times 10^{-4} \text{ erg cm}^{-2}$ . If we assume this accounts for  $\sim 1/3$  of the broadband luminosity, the total isotropic energy release is  $E_{\text{iso}} \approx 10^{54} \text{ erg}$ , comparable to that of *Sw* J1644+57 at a similar epoch. For a typical radiative efficiency for accretion power ( $\eta \equiv E_{\text{rad}}/Mc^2 \lesssim 0.1$ ), the tidal disruption of a solar-type star would require a significant beaming correction. If only a small fraction of the available energy is allocated to the observed relativistic component ( $\lesssim 1\%$ ), this would imply  $f_b \lesssim 10^{-3}$ .

In addition to the weaker degree of X-ray variability, we wish to draw attention to two other important differences be-

<sup>16</sup> The limits on the central black hole of the host galaxy of *Sw* J1644+57 are even more stringent ( $M \lesssim 10^7 M_{\odot}$ ; Levan et al. 2011; Burrows et al. 2011), and may even allow for the disruption of a white dwarf (Krolik & Piran 2011).

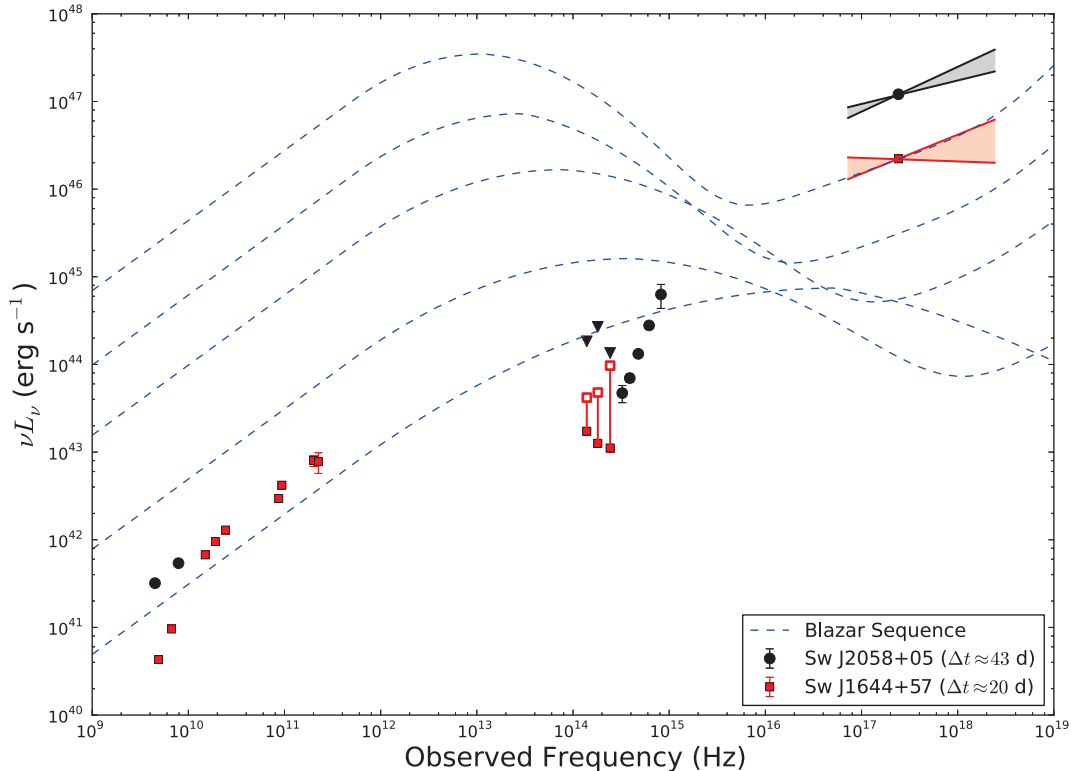


FIG. 5.— SEDs of *Sw* J2058+05 and *Sw* J1644+57, compared with the blazar “sequence” from Fossati et al. (1998). The open squares attempt to correct for the large (but uncertain) host-galaxy extinction in the case of *Sw* J1644+57 by assuming  $A_V = 5$  mag. The large X-ray luminosities of both *Sw* J2058+05 and *Sw* J1644+57 are incompatible with the observed optical and radio fluxes, which would imply an intrinsically fainter source. Both objects have complex SEDs that are difficult to reconcile with only a single emission component (e.g., synchrotron).

tween these sources. Unlike that case of *Sw* J1644+57, the observed UV/optical SED of *Sw* J2058+05 is quite blue. In fact, the rest-frame UV data for *Sw* J2058+05 can be well fit by a blackbody spectrum (Fig. 6), with  $T_{\text{BB}} \gtrsim 6 \times 10^4$  K,  $L_{\text{BB}} \gtrsim 10^{45}$  erg s $^{-1}$ , and  $R_{\text{BB}} \gtrsim 10$  AU.<sup>17</sup> The derived blackbody parameters are similar to the thermal emission observed from previous TDF candidates discovered at UV and optical wavelengths (Gezari et al. 2006, 2008, 2009; van Velzen et al. 2011; Cenko et al. 2012), and are strongly suggestive of an accretion disk origin for the optical light. In this sense, *Sw* J2058+05 may serve as a link between the bright, non-thermal X-rays observed in the relativistic TDF candidates, and the thermal disk emission from “classical” TDFs. Such comparisons were not possible for *Sw* J1644+57 due to dust in the host galaxy.

More importantly, the radio spectral index of *Sw* J2058+05 appears to be quite flat ( $f_\nu \propto \nu^0$ ). This stands in stark contrast to *Sw* J1644+57, which was optically thick ( $f_\nu \propto \nu^{1.3}$ ) up to high frequencies in the days and weeks following discovery (Zauderer et al. 2011). This may simply reflect physical differences in the jet (e.g., microphysics) or its environment (e.g., density), as is suggested by the different extinction properties. However, it may also imply a more extended (and hence long-lived) radio source, which would be difficult to reconcile with a tidal disruption origin. Future high-resolution radio interferometry (i.e., VLBI) may be able to resolve this

issue.

#### 4. IMPLICATIONS

The detection of a second member of this new class of relativistic TDFs would have important implications for the rate of these events. Given the larger redshift of *Sw* J2058+05, a significantly larger comoving volume (factor of 20) is accessible to detect analogous sources. If we adopt the local density of supermassive black holes from Tundo et al. (2007) ( $\phi \approx 10^{-3}$ – $10^{-2}$  Mpc $^{-3}$ ) and a TDF rate per galaxy of  $\sim R \times 10^{-5}$  yr $^{-1}$  ( $R \approx 1$ – $10$ ; Magorrian & Tremaine 1999; Donley et al. 2002; Esquej et al. 2007; van Velzen et al. 2011; Bower 2011), the all-sky rate of TDFs within this volume is  $R \times 10^5$  yr $^{-1}$ . Given the long-lived nature of the hard X-ray emission, it seems likely that the *Swift*-BAT would be capable of detecting similar outbursts within this volume over the entire sky during the course of its 7 years of operations to date. Thus, if all TDFs emitted similarly bright high-energy radiation isotropically, *Swift* would have detected  $\sim 7R \times 10^5$  such outbursts to date.

Given the unique X-ray light curve, it is unlikely we have confused a large number of these events with long-duration GRBs (or, for that matter, other high-energy transients). So that the observed rate is reduced by a factor of  $f_b \approx 10^{-6}$ , commensurate with having only seen two such events, we are therefore left to conclude either (1) the typical beaming fraction of these sources is extremely small ( $\theta < 1^\circ$ ), or (2) only some fraction of TDFs are capable of generating these relativistic outflows. Drawing an analogy with GRBs and core-collapse supernovae, it may be that rapid rotation of the

<sup>17</sup> Because the observed filters fall on the Rayleigh-Jeans tail, our constraints on the blackbody temperature, luminosity, and radius are essentially lower limits.

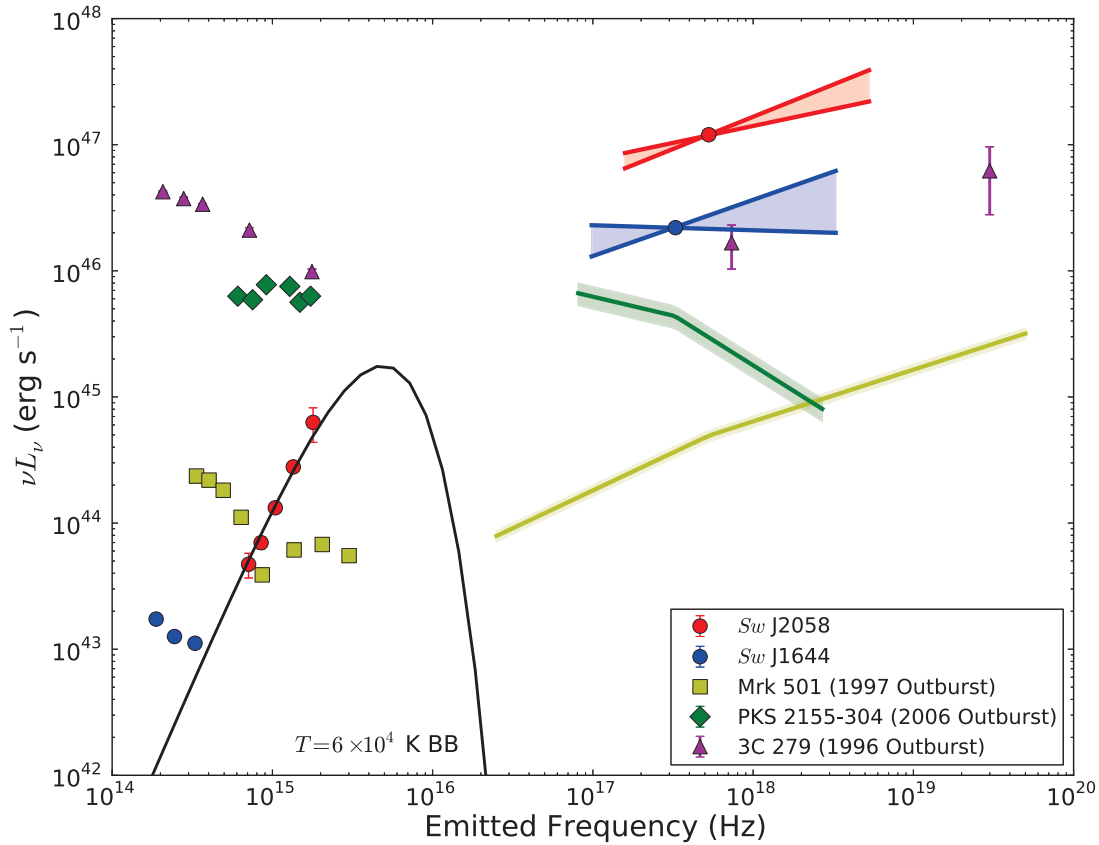


FIG. 6.— Optical and X-ray SEDs of *Sw* J2058+05 and *Sw* J1644+57, compared with some of the most dramatically variable blazars *while in outburst* (Markarian 501, Pian et al. 1998; PKS 2155-304, Foschini et al. 2007; 3C 279, Wehrle et al. 1998). Unlike any of the other objects plotted here, the rest-frame UV SED of *Sw* J2058+05 is well represented by a blackbody with  $T \approx 6 \times 10^4$  K (solid black line). We wish to thank the *Swift* PI N. Gehrels and the entire *Swift* team for their work on the remarkable facilities that enabled the discovery of this event. We thank H. Tananbaum for approving our *Chandra* ToO request (ObsID 13423), and the entire *Chandra* staff for the prompt scheduling and execution of these observations. We are grateful to G. Fosfati for providing the blazar models in tabular form, D. Poznanski for providing software to calculate the host-galaxy K-corrections, and D. Perley for assistance with the reduction of the Keck/LRIS images. We also acknowledge B. Metzger, D. Giannos, and M. Kasliwal for valuable discussions. Public data from the *Swift* data archive were used for part of this study. Some of the data presented herein were obtained at the W. M. Keck Observatory, which is operated as a scientific partnership among the California Institute of Technology, the University of California and the National Aeronautics and Space Administration; the Observatory was made possible by the generous financial support of the W. M. Keck Foundation. S.B.C. and A.V.F. acknowledge generous financial assistance from Gary & Cynthia Bengier, the Richard & Rhoda Goldman Fund, NASA/*Swift* grants NNX10AI21G and NNX12AD73G, the TABASGO Foundation, and NSF grant AST-0908886.

central black hole is required to generate *Sw* J2058+05-like events. If so, TDFs could provide a truly unique diagnostic to constrain the spin of the central black holes in distant galaxies.

Late-time radio observations should be able to distinguish between these two possibilities (Zauderer et al. 2011; Metzger et al. 2012; Berger et al. 2011). Much as has been done with long-duration GRBs (Berger et al. 2004; van der Horst et al. 2008), accurate calorimetry can be performed in the nonrelativistic regime when the outflow is spherical, bypassing any concerns about geometric corrections. Separately, the detection of off-axis events could also help address this fundamental issue (Giannios & Metzger 2011), and such searches will be greatly facilitated by future wide-field radio telescopes (e.g., LOFAR, SKA).

If, on the other hand, it is demonstrated that the emission from *Sw* J2058+05 was powered by an AGN (e.g., if repeated outbursts are detected in upcoming months and years), this would add yet another example to the already complex taxonomy of active galaxies. The rapid onset of accretion (when compared to the typical system lifetime,  $\Delta t_{\text{AGN}} \approx 10^7$  yr) would likely require some revision of our understanding of how material is channeled into the supermassive black hole, and/or the physical processes responsible for launching blazar jets. It would also greatly complicate the search for future TDFs, as standard spectroscopic diagnostic diagrams would appear to be insufficient to distinguish AGNs from normal inactive galaxies.

*Facilities:* *Swift* (BAT,XRT,UVOT), UKIRT (WFCAM), Keck:I (LRIS), Keck:II (DEIMOS), Max (GROND), WHT (ACAM)

#### REFERENCES



- , 2009b, *ApJ*, 707, L142
- Bade, N., Komossa, S., and Dahlem, M. 1996, *A&A*, 309, L35
- Barthelmy, S. D., et al. 2005, *Space Science Reviews*, 120, 143
- Becker, R. H., White, R. L., and Helfand, D. J. 1995, *ApJ*, 450, 559
- Berger, E., Kulkarni, S. R., and Frail, D. A. 2004, *ApJ*, 612, 966
- Berger, E., Zauderer, A., Pooley, G. G., Soderberg, A. M., Sari, R., Brunthaler, A., and Bietenholz, M. F. 2011, arXiv e-prints (astro-ph/1112.1697)
- Bloom, J. S., et al. 2011, *Science*, 333, 203
- Bower, G. C. 2011, *ApJ*, 732, L12
- Brandt, W. N., Pounds, K. A., and Fink, H. 1995, *MNRAS*, 273, L47
- Burrows, D. N., et al. 2011, *Nature*, 476, 421
- Burrows, D. N., et al. 2005, *Space Science Reviews*, 120, 165
- Butler, N. R. and Kocevski, D. 2007, *ApJ*, 663, 407
- Campana, S., Foschini, L., Tagliaferri, G., Ghisellini, G., and Covino, S. 2011, *GRB Coordinates Network*, 1851
- Cannizzo, J. K., Troja, E., and Lodato, G. 2011, *ApJ*, 742, 32
- Cenko, S. B., et al. 2012, *MNRAS*, 2203
- Condon, J. J., Cotton, W. D., Greisen, E. W., Yin, Q. F., Perley, R. A., Taylor, G. B., and Broderick, J. J. 1998, *AJ*, 115, 1693
- Donley, J. L., Brandt, W. N., Eracleous, M., and Boller, T. 2002, *AJ*, 124, 1308
- Esquej, P., Saxton, R. D., Freyberg, M. J., Read, A. M., Altieri, B., Sanchez-Portal, M., and Hasinger, G. 2007, *A&A*, 462, L49
- Esquej, P., et al. 2008, *A&A*, 489, 543
- Evans, P. A., et al. 2009, *MNRAS*, 397, 1177
- Faber, S. M., et al. 2003, in *Society of Photo-Optical Instrumentation Engineers (SPIE) Conference Series*, Vol. 4841, *Society of Photo-Optical Instrumentation Engineers (SPIE) Conference Series*, ed. M. Iye & A. F. M. Moorwood, 1657–1669
- Filippenko, A. V. 1982, *PASP*, 94, 715
- Foschini, L., et al. 2011, *MNRAS*, 413, 1671
- , 2007, *ApJ*, 657, L81
- Fossati, G., et al. 2008, *ApJ*, 677, 906
- Fossati, G., Maraschi, L., Celotti, A., Comastri, A., and Ghisellini, G. 1998, *MNRAS*, 299, 433
- Gehrels, N., et al. 2004, *ApJ*, 611, 1005
- Gezari, S., et al. 2006, *ApJ*, 653, L25
- , 2008, *ApJ*, 676, 944
- , 2009, *ApJ*, 698, 1367
- Giannios, D. and Metzger, B. D. 2011, *MNRAS*, 416, 2102
- Goad, M. R., et al. 2008, *A&A*, 492, 873
- Greiner, J., et al. 2008, *PASP*, 120, 405
- Greiner, J., Schwarz, R., Zharikov, S., and Orio, M. 2000, *A&A*, 362, L25
- Grupe, D., Beuermann, K., Mannheim, K., Bade, N., Thomas, H., de Martino, D., and Schwope, A. 1995, *A&A*, 299, L5
- Gültekin, K., Cackett, E. M., Miller, J. M., Di Matteo, T., Markoff, S., and Richstone, D. O. 2009, *ApJ*, 706, 404
- Ho, L. C. 2009, *ApJ*, 699, 626
- Horne, K. 1986, *PASP*, 98, 609
- Kalberla, P. M. W., Burton, W. B., Hartmann, D., Arnal, E. M., Bajaja, E., Morras, R., and Pöppel, W. G. L. 2005, *A&A*, 440, 775
- Kann, D. A., et al. 2010, *ApJ*, 720, 1513
- Kelson, D. D. 2003, *PASP*, 115, 688
- Kinney, A. L., Calzetti, D., Bohlin, R. C., McQuade, K., Storchi-Bergmann, T., and Schmitt, H. R. 1996, *ApJ*, 467, 38
- Komossa, S. and Greiner, J. 1999, *A&A*, 349, L45
- Krimm, H. A., et al. 2011, *The Astronomer's Telegram*, 3384
- Krolik, J. H. and Piran, T. 2011, *ApJ*, 743, 134
- Kulkarni, S. R., et al. 1998, *Nature*, 395, 663
- Lauer, T. R., et al. 2007, *ApJ*, 662, 808
- Levan, A. J., et al. 2011, *Science*, 333, 199
- Magorrian, J. and Tremaine, S. 1999, *MNRAS*, 309, 447
- Magorrian, J., et al. 1998, *AJ*, 115, 2285
- Maksym, W. P., Ulmer, M. P., and Eracleous, M. 2010, *ApJ*, 722, 1035
- Metzger, B. D., Giannios, D., and Mimica, P. 2012, *MNRAS*, 2207
- Miller, J. M. and Gültekin, K. 2011, *ApJ*, 738, L13
- Murray, S. S., et al. 1997, in *Society of Photo-Optical Instrumentation Engineers (SPIE) Conference Series*, Vol. 3114, *Society of Photo-Optical Instrumentation Engineers (SPIE) Conference Series*, ed. O. H. Siegmund & M. A. Gummin, 11–25
- Oke, J. B. and Gunn, J. E. 1983, *ApJ*, 266, 713
- Oke, J. B., et al. 1995, *PASP*, 107, 375
- Perley, R. A., Chandler, C. J., Butler, B. J., and Wrobel, J. M. 2011, *ApJ*, 739, L1
- Pian, E., et al. 2007, *ApJ*, 664, 106
- , 1998, *ApJ*, 492, L17
- Pineau, F.-X., Motch, C., Carrera, F., Della Ceca, R., Derrière, S., Michel, L., Schwope, A., and Watson, M. G. 2011, *A&A*, 527, A126
- Poole, T. S., et al. 2008, *MNRAS*, 383, 627
- Rau, A., Greiner, J., and Olivares, F. 2011a, *The Astronomer's Telegram*, 3390
- Rau, A., Greiner, J., Schady, P., Olivares, F., Krimm, H., and Holland, S. 2011b, *The Astronomer's Telegram*, 3425
- Readhead, A. C. S. 1994, *ApJ*, 426, 51
- Rees, M. J. 1988, *Nature*, 333, 523
- Remillard, R. A. and McClintock, J. E. 2006, *ARA&A*, 44, 49
- Renzini, A., Greggio, L., di Serego Alighieri, S., Cappellari, M., Burstein, D., and Bertola, F. 1995, *Nature*, 378, 39
- Roming, P. W. A., et al. 2005, *Space Science Reviews*, 120, 95
- Schlegel, D. J., Finkbeiner, D. P., and Davis, M. 1998, *ApJ*, 500, 525
- Skrutskie, M. F., et al. 2006, *AJ*, 131, 1163
- Socrates, A. 2011, arXiv e-prints (astro-ph/1105.2557)
- Spergel, D. N., et al. 2007, *ApJS*, 170, 377
- Tundo, E., Bernardi, M., Hyde, J. B., Sheth, R. K., and Pizzella, A. 2007, *ApJ*, 663, 53
- Urry, C. M. and Padovani, P. 1995, *PASP*, 107, 803
- van der Horst, A. J., et al. 2008, *A&A*, 480, 35
- van Velzen, S., et al. 2011, *ApJ*, 741, 73
- Véron-Cetty, M.-P. and Véron, P. 2010, *A&A*, 518, A10
- Voges, W., et al. 1999, *A&A*, 349, 389
- Wehrle, A. E., et al. 1998, *ApJ*, 497, 178
- Zauderer, B. A., et al. 2011, *Nature*, 476, 425

TABLE 1  
UV/OPTICAL/NIR OBSERVATIONS OF *Sw* J2058+05

Date <sup>a</sup> (2011 UT)	Telescope/Instrument	Filter	Exposure Time (s)	Magnitude <sup>b</sup>
May 27.91	UVOT	<i>b</i>	2927.3	> 21.50
May 28.38	GROND	<i>J</i>	720.0	> 19.6
May 28.38	GROND	<i>H</i>	720.0	> 19.0
May 28.38	GROND	<i>K</i>	720.0	> 17.3
May 29.41	GROND	<i>g'</i>	3600.0	22.55 ± 0.06
May 29.41	GROND	<i>r'</i>	3600.0	22.66 ± 0.07
May 29.41	GROND	<i>i'</i>	3600.0	22.89 ± 0.18
May 29.41	GROND	<i>z'</i>	3600.0	22.91 ± 0.27
May 29.41	GROND	<i>J</i>	3600.0	> 21.0
May 29.41	GROND	<i>H</i>	3600.0	> 20.5
May 29.41	GROND	<i>K</i>	3600.0	> 18.0
May 30.58	UVOT	<i>uvw1</i>	2580.1	> 22.80
Jun 2.41	UVOT	<i>uvm2</i>	2889.8	> 23.07
Jun 3.40	GROND	<i>g'</i>	1440.0	22.57 ± 0.06
Jun 3.40	GROND	<i>r'</i>	1440.0	22.68 ± 0.09
Jun 3.40	GROND	<i>i'</i>	1440.0	22.81 ± 0.15
Jun 3.40	GROND	<i>z'</i>	1440.0	23.20 ± 0.34
Jun 3.40	GROND	<i>J</i>	1440.0	> 21.4
Jun 3.40	GROND	<i>H</i>	1440.0	> 20.9
Jun 3.40	GROND	<i>K</i>	1440.0	> 18.8
Jun 5.88	UVOT	<i>uvw2</i>	3059.2	> 23.37
Jun 8.57	UVOT	<i>u</i>	2258.0	21.51 ± 0.29
Jun 10.26	GROND	<i>g'</i>	9600.0	22.40 ± 0.05
Jun 10.26	GROND	<i>r'</i>	9600.0	22.62 ± 0.06
Jun 10.26	GROND	<i>i'</i>	9600.0	22.98 ± 0.11
Jun 10.26	GROND	<i>z'</i>	9600.0	23.17 ± 0.20
Jun 10.26	GROND	<i>J</i>	9600.0	> 21.9
Jun 10.26	GROND	<i>H</i>	9600.0	> 21.2
Jun 10.26	GROND	<i>K</i>	9600.0	> 19.3
Jun 14.04	UVOT	<i>uvm2</i>	3113.3	> 23.13
Jun 17.11	UVOT	<i>uvw2</i>	2823.8	> 23.43
Jun 18.51	WFCAM	<i>H</i>	2400.0	> 20.8
Jun 18.53	WFCAM	<i>K</i>	2400.0	> 20.9
Jun 23.54	UVOT	<i>uvw1</i>	2434.2	> 22.92
Jun 26.55	UVOT	<i>uvm2</i>	2468.0	> 23.12
Jun 29.45	Keck/LRIS	<i>g'</i>	300.0	22.75 ± 0.04
Jun 29.45	Keck/LRIS	<i>R</i>	280.0	22.82 ± 0.04
Jul 1.76	UVOT	<i>uvw1</i>	3050.1	> 23.02
Jul 6.46	UVOT	<i>u</i>	2402.1	22.09 ± 0.29
Jul 7.00	UVOT	<i>uvw2</i>	430.1	> 22.21
Jul 9.15	WHT	<i>r'</i>	300.0	22.96 ± 0.04
Jul 9.17	WHT	<i>g'</i>	300.0	23.02 ± 0.05
Jul 11.53	UVOT	<i>uvw2</i>	2271.5	> 23.36

<sup>a</sup>UT at beginning of exposure.

<sup>b</sup>Reported magnitudes have not been corrected for Galactic extinction ( $E(B - V) = 0.095$  mag; Schlegel *et al.* 1998). Upper limits represent  $3\sigma$  uncertainties.